



Functionalized magnesium alloys obtained by superplastic forming process retain osteoinductive and antibacterial properties: An in-vitro study

Marco Tatullo^{a,*}, Adriano Piattelli^b, Roberta Ruggiero^c, Rosa Maria Marano^c, Flavia Iaculli^d, Carlo Rengo^d, Ida Papallo^e, Gianfranco Palumbo^f, Roberto Chiesa^g, Francesco Paduano^c, Gianrico Spagnuolo^{d,*}

^a Department of Translational Biomedicine and Neuroscience, School of Medicine, University of Bari "Aldo Moro", 70124 Bari, Italy

^b School of Dentistry, Saint Camillus International University of Health and Medical Sciences, 00131 Rome, Italy

^c Stem Cells and Medical Genetics Units, Tecnologica Research Institute and Marrelli Health, 88900 Crotone, Italy

^d Department of Neurosciences, Reproductive and Odontostomatological Sciences, University of Naples Federico II, via S. Pansini 5, 80131 Naples, Italy

^e CeSMA, University of Naples Federico II, Corso Nicolangelo Prototipisani, 80146 Naples, Italy

^f Department of Mechanics, Polytechnic University of Bari, 70124 Bari, Italy

^g Department of Chemistry, Materials and Chemical Engineering 'G. Natta', Politecnico di Milano, 20135 Milan, Italy

ARTICLE INFO

Keywords:

Antibacterial materials
Bone tissue engineering
Mg alloys
Metallic biomaterials
Resorbable implants

ABSTRACT

Objectives: This study aimed to investigate the biocompatibility, osteogenic and antibacterial activity of biomedical devices based on Magnesium (Mg) Alloys manufactured by Superplastic Forming process (SPF) and subjected to Hydrothermal (HT) and Sol-Gel Treatment (Sol-Gel).

Methods: Mg-SPF devices subjected to Hydrothermal (Mg-SPF+HT) and Sol-Gel Treatment (Mg-SPF+Sol-Gel) were investigated. The biocompatibility of Mg-SPF+Sol-Gel and Mg-SPF+HT devices was observed by indirect and direct cytotoxicity assays, whereas the colonization of sample surfaces was assessed by confocal microscopy. qRT-PCR analysis and microbial growth curve analyses were employed to evaluate the osteogenic and antibacterial activity of both SPF-Mg treated devices, respectively.

Results: Mg-SPF+HT and Mg-SPF+Sol-Gel showed a high degree of biocompatibility. Analysis of mRNA expression of osteogenic genes in cells cultured on Mg-treated devices revealed a significant upregulation of the expression levels of *BMP2* and *Runx-2*. Furthermore, the bacterial growth in strains developed in contact with both the Mg-SPF+HT and Mg-SPF+Sol-Gel devices was lower than that observed in the control.

Significance: Hydrothermal and Sol-Gel Treatments of Mg alloys obtained through the SPF process demonstrated bioactive, osteogenic and antibacterial activity, offering a promising alternative to conventional Mg-based devices. The obtained Mg-based materials may have the potential to enhance the tunability of temporary devices in maxillary reconstruction, eliminating the need for second surgeries, and ensuring a good bone reconstruction and a reduced implant failure rate due to bacterial infections.

1. Introduction

Metallic biomaterials, due to their high strength, toughness, ease of processing, and good biocompatibility, are considered a gold standard in dental implantology [1,2]. Among the metallic biomaterials, Magnesium (Mg) and its alloys have gained growing attention in numerous clinical settings, thanks to their ability to differently degrade in several biological environments [3].

Literature has reported that Mg alloys may be considered an excellent choice for complex surgical procedures involving the restoration of clinical functions in maxillary bones through bone regeneration; this is especially relevant in cases of trauma or tissue loss [3,4]. Mg is a bioactive element, commonly found in cells and bone tissues where it supports osteoinductive and osteoconductive processes. Nonetheless, a notable drawback of Mg is its rapid corrosion under specific conditions, such as the presence of certain biological fluids or exposure to aggressive

Abbreviations: BTE, Bone Tissue Engineering; Mg, Magnesium; SPF, Superplastic Forming; HT, Hydrothermal Treatment; hPCy-MSCs, human Periapical Cysts-Mesenchymal Stem Cells; OD, Optical Density.

* Corresponding authors.

E-mail addresses: marco.tatullo@uniba.it (M. Tatullo), gspagnuolo@unina.it (G. Spagnuolo).

<https://doi.org/10.1016/j.dental.2024.01.005>

Received 1 September 2023; Received in revised form 28 January 2024; Accepted 31 January 2024

Available online 7 February 2024

0109-5641/© 2024 The Author(s). Published by Elsevier Inc. on behalf of The Academy of Dental Materials. This is an open access article under the CC BY license (<http://creativecommons.org/licenses/by/4.0/>).

stress [5]. Innovative coating technologies, such as electrochemical plating and anodizing, have been developed to overcome impacting limitations related to corrosion [5,6]. In addition, novel manufacturing procedures have been redirected from the aerospace industry to biomedical devices.

The potential of controlling the process–structure–property relationship for a material takes a fundamental role in the development of biomedical devices with desired features at different levels.

In particular, the relationship among process parameters, chemical composition, microstructural features, mechanical and biological properties is of paramount interest in the biomedical field, involving several technological areas (e.g., plastic forming, casting, sintering) as well as the combination of both traditional and advanced methods.

Superplastic forming (SPF) is a specialized metal forming process that involves the ability of certain materials to undergo significant elongation (deformation) without tearing or fracture under specific conditions of temperature and strain rate. SPF is widely recognized as an effective technique to mitigate the low formability challenges encountered at elevated temperatures. Literature has reported that the optimization of the forming process is sensitive to microstructure degradation mechanisms, and SPF may control the Mg-alloys degradation in multi-sheet materials [7]. This study aimed to investigate if Magnesium Alloys (MA) devices manufactured by SPF and subjected to Hydrothermal (Mg-SPF+HT) and Sol-Gel (Mg-SPF+Sol-Gel) treatment exhibit biocompatibility as well as osteogenic and antibacterial activity.

2. Materials and methods

2.1. Samples preparation

The samples investigated in this work were Mg-based implant surfaces, manufactured utilizing the Superplastic Forming (SPF) process. Briefly, Mg-SPF samples were obtained using the equipment, available at the Polytechnic University of Bari. It's composed of two tools placed into a shell furnace, which allows to reach a uniform temperature: the upper die acts as a blankholder while the lower one as the shaped die. The Mg disks ($d=75$ mm) to be deformed were put between the tools, when the proper process temperature was reached (450 °C), and were clamped setting the blankholder force to prevent any material drawing. The pressurized gas (argon), which was inflated according to a specific profile (calculated using finite element simulations implementing the material superplastic properties), compelled the blank to copy the shape of the bottom tool. To maximize the number of flat samples to be extracted after SPF, taking into account the geometrical constraint on the maximum diameter of the shell furnace, squared flat samples (9 mm \times 9 mm) were cut from the bottom part of the superplastically formed component.

SPF uncoated Mg samples were treated by Hydrothermal Treatment (Mg-SPF+HT), soaking the samples in distilled water inside an autoclave at 160 °C for 4; this treatment produced a homogenous magnesium hydroxide $Mg(OH)_2$ coating, about 20 micrometers thick, on the surface of the samples.

Sol-gel coating technique was also considered to deposit a thin $Mg(OH)_2$ layer on the surface of SPF-Mg samples. Sol-gel coatings (Mg-SPF+Sol-Gel) were obtained by dipping untreated SPF-Mg samples into a solution containing the nanoparticles of $Mg(OH)_2$ and the (3-glycidypropyl)-trimethoxysilane (GLYMO), that was used to achieve better adhesion to the SPF-Mg samples. First, a 2.2 M NH_4OH solution was added drop by drop to a 0.4 M $MgCl_2$ solution to obtain $Mg(OH)_2$ nanoparticles. The silane solution was prepared by mixing GLYMO, 2-propanol, and distilled water with a volume ratio of 8:8:1. Subsequently, the $Mg(OH)_2$ solution and GLYMO solution were mixed and kept under magnetic stirring for 2 h. Dip-coated samples were thermal treated in the oven at 160 °C for 2 h. Uncoated Mg samples were obtained by cutting components formed by the SPF forming technique from AZ31 sheets.

2.2. Indirect cytotoxicity assay

The biocompatibility was tested according to scientific literature and following the ISO 10993–12 and the ISO 10993–5 guidelines [7,8]. Specifically, murine fibroblast cells (L929) were cultured until confluency; then, confluent clustered cells were treated with trypsin and seeded into 96-well plates at a density of 3×10^3 cells/150 μ L. The plates were incubated at 37 °C with 5% CO_2 . To prepare the extract/conditioned mediums (CM), the metal samples were cleaned, sterilised, and incubated in DMEM complete medium for 72 h. 0.2 g of Mg devices for 10 mL of DMEM (0.2 g/mL) was considered to obtain the CM. Then, the supernatant fluid was filtered by a 0.2 μ m filter before starting the cytotoxicity test. After 72 h, the media were replaced with 100 μ L of the extract media. 10% dimethyl sulfoxide (DMSO) (100 μ L/well) and DMEM medium alone (100 μ L/well) were used as positive and negative controls, respectively. The cytotoxicity evaluation of each sample was performed using the PrestoBlue® assay (Thermo Fisher) after 1, 3, and 7 days. Specifically, a 1X PrestoBlue solution was added at a concentration of 100 μ L/well and incubated for 4 h. The absorbance was measured at two different wavelengths: 570 nm and 600 nm, by a Multiskan GO Microplate Spectrophotometer (Thermo Scientific). The Mg-based samples used for the indirect cytotoxicity assay were configured in a square shape with dimensions of 9×9 mm.

2.3. Direct cytotoxicity assay

Human periapical cyst-mesenchymal stem cells (hPCy-MSCs), which have been demonstrated to hold osteogenic commitment [9], were seeded onto 6 different samples (three for each group) at a density of 1×10^4 cells/60 μ L and incubated for 1 h at 37 °C and 5% CO_2 to allow adhesion. After 1 h, 1 mL of alpha-MEM complete was added to each scaffold. Cells cultured on 24-well plates at the same density served as control. The proliferation rate of hPCy-MSCs cultured on Mg-SPF+Sol-Gel and Mg-SPF+HT was assessed with viability reagent PrestoBlue® (Thermo Fisher) for 2, 4 and 7 days. The Mg-based samples used for the direct cytotoxicity assay were configured in a square shape with dimensions of 9×9 mm.

2.4. Cell viability assay

The colonisation of the Mg devices (Mg SPF+Sol-Gel and Mg-SPF+HT) was assessed using the Cell Viability assay (Biotium) and confocal microscopy. Specifically, 1×10^4 hPCy-MSCs were seeded onto the implant surfaces (three for each group) and incubated in alpha-MEM complete medium for 7 days. Then, cells were incubated at 37 °C with green fluorescence (Calcein-AM) and red fluorescence (Ethidium Homodimer III - EthD-III) to detect live and dead cells, respectively. The samples were also analysed through confocal microscopy. The Mg-based samples used for the cell viability assay were configured in a square shape with dimensions of 9×9 mm.

2.5. Gene expression analysis

To assess the osteogenic/osteoinductive properties of Mg-SPF+Sol-Gel and Mg-SPF+HT, the real-time PCR (qRT-PCR) analysis was used to evaluate osteogenesis-related gene expressions. To achieve this objective, 1×10^4 human Periapical Cysts-Mesenchymal Stem Cells (hPCy-MSCs) [9] were cultured on both experimental devices. Briefly, the RNA was extracted from hPCy-MSCs after 14 days of culture on Mg devices; the RNA extracted from hPCy-MSCs growth on a plastic surface has been used as a control (CTR). The RNA extracted was quantified by spectrophotometry and diluted to 100 ng/ μ L with RNAase/DNAse free water. Following, 500 ng of RNA were transcribed in cDNA by using reverse transcriptase *Hg-capacity RNA to cDNA kit*. Then, a PCR mix containing the Taq (*Taqman Universal master mix*, Thermo Fischer), the primers of genes *COL1A1*, *BMP2*, *ALP*, *NF-kb*, *RUNX-2*, *RUNK* and each specific

probe (Taqman gene expression assay) was prepared. The qRT-PCR was performed with the instrument piKoreal (Thermo Scientific) as follows: (a) 95 °C for 10 min (Taq activation); (b) 95 °C for 15 s (Denaturation); and (c) 60 °C for 1 min (Annealing/Extension). Gene expression levels were calculated using the comparative CT method ($\Delta\Delta C_t$) by normalizing respect to glyceraldehyde-3-phosphate dehydrogenase (GAPDH) gene expression. The TaqMan primers were used as follows: *collagen type I alpha I* (COL1A1), Hs01076775_g1; *RANK* (TNFRSF11A), Hs00921374_m1; *NFkB*, Hs00428211_m1; *Runt-related transcription factor 2* (RUNX2), Hs00231692_m1; *alkaline phosphatase* (ALP), Hs00758162_m1; *Bone morphogenetic protein 2* (BMP-2), Hs00154192_m1; and (*GAPDH*), Hs99999905_m1 (Thermo Fischer).

2.6. Antibacterial activity

The antibacterial activity of Mg-based functionalized devices (Mg-SPF+Sol-Gel and Mg-SPF+HT) was investigated by using an *Enterobacter* strain according to the methods used by Choi et al. [10]. More in detail, the bacterial suspension of *Enterobacter* (*Salmonella typhimurium*) was cultured overnight. To obtain an optical density (OD) of 0.02 at 600 nm, the bacterial culture broth was modified accordingly. Then, the Mg-SPF+Sol-Gel and Mg-SPF+HT devices were immersed in 3 mL of bacterial culture broth and incubated at 37 °C, under continuous shaking. The bacterial growth was detected by monitoring the state of turbidimetry; a spectrophotometer (Multiskan GO, Thermo Scientific) was used to investigate the bacterial growth at different times (0, 6, 24 and 30 h).

2.7. Statistical analysis

A statistical comparison was performed between the tested groups and the controls using one-way analysis of variance (ANOVA) with GraphPad Prism 6 software (GraphPad Software Inc., San Diego, CA, USA). Significance for all statistical analyses was defined as $P < 0.05$ (*), $P < 0.01$ (**), $P < 0.005$ (***), $P < 0.001$ (****). In all experiments, three measurements were considered, to obtain the results as mean \pm

standard deviation.

3. Results

3.1. Cytotoxicity activity

The biocompatibility of Mg-SPF+Sol-Gel and Mg-SPF+HT samples was demonstrated, as summarised in Fig. 1. To prepare the conditioned medium, samples were cleaned, sterilised and incubated in DMEM medium for 72 h (Fig. 1A). Then, the indirect cytotoxicity was investigated, according to ISO 10993–12 and ISO 10993–5 guidelines. The graphs (Fig. 1B) show the cell viability values of L929 cells cultured for 1, 3 and 7 days in CM obtained by immersion of Mg-SPF+Sol-Gel and Mg-SPF+HT devices. All the experimental samples were compared to uncoated samples. Cell viability reached values around 100% in both Mg-SPF+Sol-Gel and Mg-SPF+HT devices, demonstrating a highly significant cytocompatibility.

Additionally, cell growth and proliferation of hPCy-MSCs on Mg-SPF+Sol-Gel and Mg-SPF+HT through in-vitro proliferation assays and fluorescence microscopy were investigated. The growing trend of hPCy-MSCs cultured on Mg SPF+Sol-Gel and Mg-SPF+HT samples for 2, 4 and 7 days is reported in Fig. 2. The absorbance values, indicative of the metabolic activity of cells, demonstrated an increasing trend over time, suggesting that cells were fully viable and proliferating at the 3-time points (Fig. 2A). In addition, Cell Viability assay (Biotium) and confocal microscopy investigations were used to assess the colonization of the Mg devices. Specifically, cells were incubated with Calcein-AM and Ethidium Homodimer III (EthD-III) and high levels of cell viability were reported (Fig. 2B). In addition, the results of the statistical analysis showed that there was no statistically significant difference in cell viability between the Mg-SPF+Sol-Gel and Mg-SPF+HT devices.

3.2. Gene expression analysis

The mRNA expression levels of osteogenic genes in cells cultured for 14 days on the two types of Mg coatings (Mg-SPF+Sol-Gel and Mg-

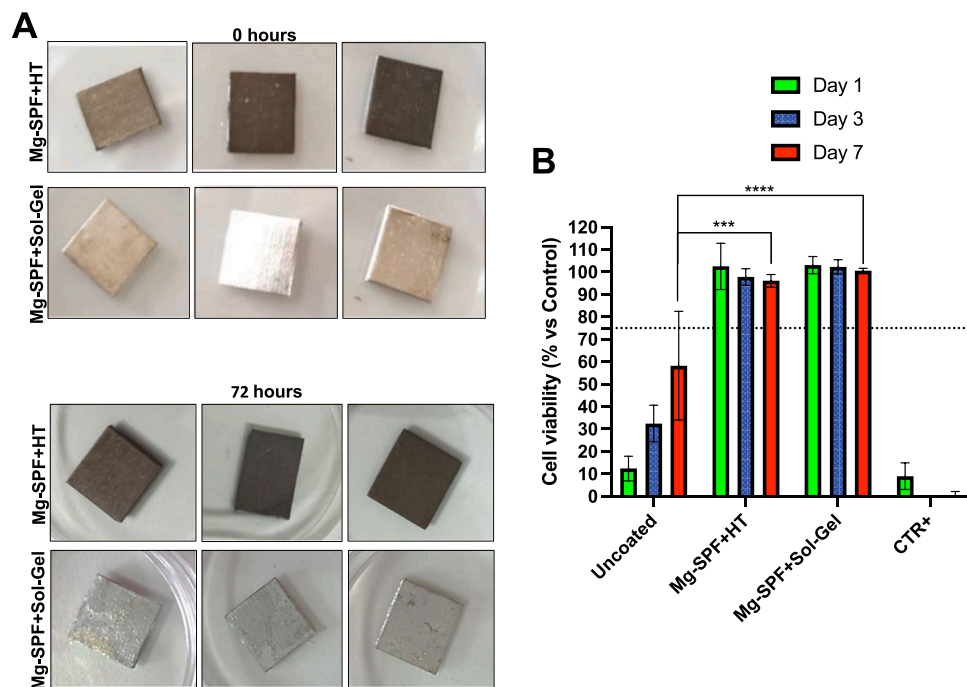


Fig. 1. Indirect cytotoxicity assay of Mg-SPF+Sol-Gel and Mg-SPF+HT. (A) Samples on two different time points of the extraction phase ($T = 0$ h and $T = 72$ h). (B) Proliferation assessment (% vs control) of L929 grown in the extract media obtained from Mg-SPF+Sol-Gel and Mg-SPF+HT performed on 1, 3 and 7 days. *** $P < 0.005$, **** $P < 0.001$.

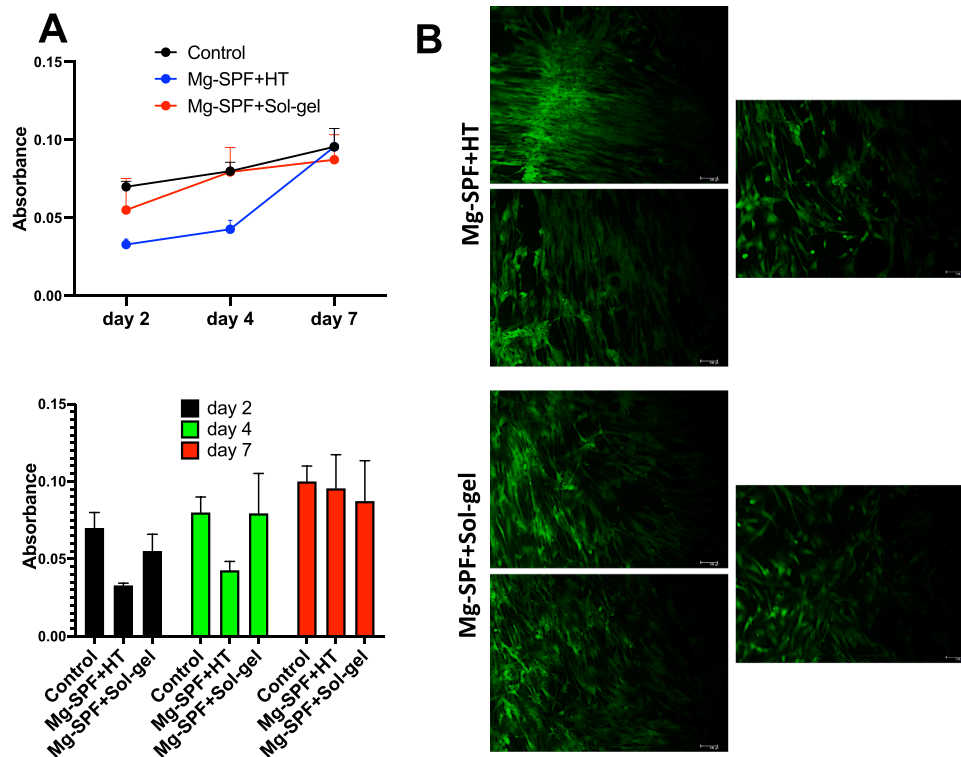


Fig. 2. Cytotoxicity assessment by direct contact. (A) Metabolic activity of hPCy-MSCs cultured on Mg-SPF+Sol-Gel e Mg-SPF+HT specimens for 2, 4 and 7 days was evaluated with PrestoBlue assay. (B) Live/Dead assay of hPCy-MSCs seeded on Mg-SPF+Sol-Gel and Mg-SPF+HT devices was performed after 7 days; green represents live cells.

SPF+HT) are shown in Fig. 3. The expression levels of *BMP2* were significantly upregulated in cells cultured on Mg-SPF+HT and Mg-SPF+Sol-Gel devices compared to the control. However, the expression levels of *Col1A1* and *ALP* were found to be markedly reduced in cells cultured on Mg-SPF+HT and Mg-SPF+Sol-Gel devices. The gene expression levels of *Runx-2* were significantly higher in cells cultured on both the Mg-SPF+Sol-Gel and Mg-SPF+HT devices with respect to control. Notably, the results showed that there was a positive correlation between the expression levels of *BMP2* and *Runx2* in cells cultured on both types of Mg coatings. Furthermore, the expression levels of *NFκB*

and *RUNK* in hPCy-MSCs cultured on Mg-SPF+HT and Mg-SPF+Sol-Gel devices were increased compared to the control, although no statistical differences were observed.

3.3. Antibacterial activity

The bacterial growth in strains developed in contact with both the Mg-SPF+HT and Mg-SPF+Sol-Gel devices was lower than the bacterial growth observed in the control (Fig. 4). The functionalized Mg-based devices showed interesting antimicrobial bioactivity (Fig. 3A). Importantly, after 30 h the inhibition of bacterial growth induced by Mg-SPF+HT and Mg-SPF+Sol-Gel devices was significantly higher than those observed in the control (Fig. 3B). These results suggest that both Mg-treated devices can be considered as potential antibacterial materials for biomedical applications.

4. Discussion

Mg alloy properties make them smart and able to be translated into several tissue engineering and biomedical applications. They have been widely investigated, developed, and employed in artificial joints, spinal rehabilitation, and oral implants [11,12]. Mg holds notable characteristics, including biocompatibility, biodegradability, and full resorbability [11]. Extensive in vitro and in vivo studies have been aimed to limit the corrosion of Mg and its alloys [3,4]. Nevertheless, the high corrosion rate of these biomaterials remains an issue that affects the predictability of these resorbable implants in medical procedures. To face this limitation, the surface modification of Mg alloys has been suggested in several studies, as it may be considered a versatile strategy to both reduce uncontrolled corrosion and enhance osteogenic and antibacterial properties [13–17]. This study evaluated the behavior of specific Mg-based devices manufactured by the SPF process and functionalized with different coatings to improve their surface bioactivity, preventing implant-related infections and improving osteogenesis [18].

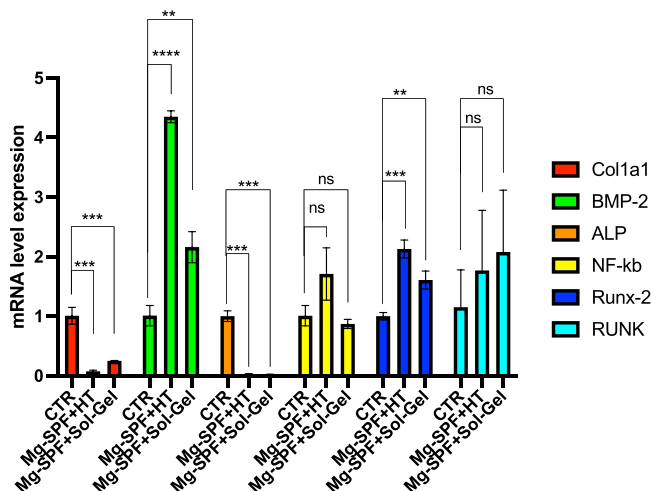


Fig. 3. Gene expression analysis. Osteogenic capabilities of different coatings using orally derived mesenchymal stem cells (MSCs). mRNA expression levels assessment of *NFκB*, *COL1A1*, *BMP-2*, *ALP*, *RANK* e *Runx-2* in hPCy-MSCs cultured on Mg-SPF+Sol-Gel and Mg-SPF+HT for 14 days. * $P < 0.01$, *** $P < 0.005$, **** $P < 0.001$, ns (not significant).

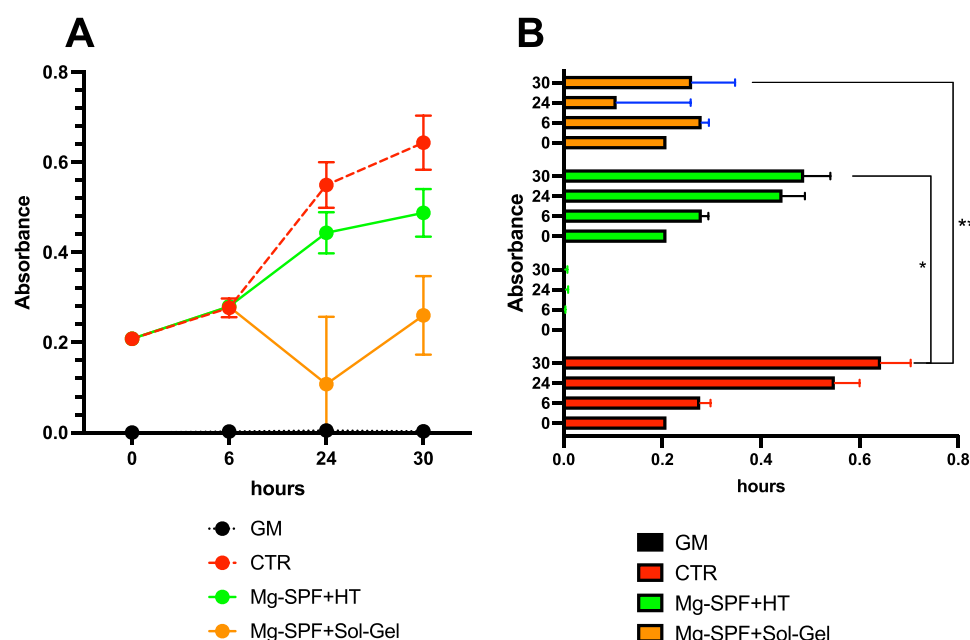


Fig. 4. Antimicrobial bioactivity of Mg-treated devices. (A) Microbial growth curves of *Enterobacter* (*Salmonella typhimurium*) in contact with Mg-SPF+Sol-Gel and Mg-HT at different time points. (B) Histogram of *Salmonella typhimurium* microbial growth in contact with Mg-SPF-Sol-Gel and Mg-HT samples measured at 0, 6, 24, and 30 h. Optical density (OD) at 600 nm was used to monitor the analysis of growth curves. CTR, control (*Enterobacter* only); GM (Growth Medium) bacterial growth medium only; Mg-Sol-gel, SPF Mg device subjected to Sol-Gel treatment; Mg-HT, SPF Mg device subjected to HT treatment. * $P < 0.05$, * * $P < 0.01$.

In the present study study, the hydrothermal treatment to increase the resistance to Mg corrosion, and the Sol-Gel coating made of a zirconia matrix doped with metallic cations to reduce bacterial infections were adopted. Sol-Gel coating is advantageous, due to its low processing temperature, high purity, and homogeneity [19–21].

The study demonstrated that L929 cells were viable on Mg-coated implants, as they exhibited homogeneous colonization of both Mg SPF+Sol-Gel and Mg-SPF+HT devices. Additionally, qRT-PCR analysis was used to evaluate osteogenesis-related gene expressions, focusing on markers such as *BMP-2* and *Runx-2* [22–24]. The observed results have further confirmed the osteogenic capabilities of these Mg-coated samples, strategic for dental implantology [25,26]. Accordingly, other studies, involving coatings on Mg alloy surfaces with hydroxyapatite and *BMP-2* have similarly demonstrated good biocompatibility and osteogenesis [27–31].

Finally, the still unsolved issue of implant infections has attracted interest in the antibacterial properties exhibited by Mg-based prosthetic implants [32–38]. The present study has shown that the investigated Mg devices, functionalized as previously described (Mg-SPF+Sol-Gel and Mg-SPF+HT), were able to exert antimicrobial activity against *Salmonella typhimurium*.

However, the current research demonstrated potential limitations such as (i) the lack of analysis concerning degradation and/or corrosion rates and related mechanisms; and ii) the absence of mechanical characterization to understand the effect of the proposed functionalization strategies, which should provide further insight into the functional features of the designed devices, and iii) the antibacterial activity of Mg-treated devices evaluated only against *Salmonella typhimurium*.

In conclusion, the present research offers valuable insights into the potential of Mg-based materials for the development of advanced biodegradable implants, showcasing their enhanced biocompatibility, osteogenic and antibacterial activity. These findings pave the way for future advancements in orthopedic and dental applications, as Mg-based materials continue to demonstrate their revolutionary promise in treating refractory bone diseases and infections.

Moreover, it is also worth remembering that the current interest in advanced design strategies and technologies, such as additive

manufacturing (i.e., 3D printing), is widely increasing in surgical and medical fields, with the scope to develop innovative and patient-specific implants with adequate performances. Indeed, benefiting from the obtained results, the current research would also represent a further study toward future work to design and fabricate complex, customized Mg-based porous devices, characterized by additively manufactured lattice structures with tailored morphology, and mechanical and functional properties.

5. Conclusions

Within the limitations of the current research analyzing the combination of SPF-Mg alloys functionalized with two of the most promising coatings applied on Mg-based biomedical devices, the following conclusions were reached:

1. the Mg-based devices, here surface-functionalized (i.e., HT and Sol-Gel treatment), may promote osteogenesis at the implant interface;
2. the adopted design and functionalization strategies led to advanced devices (i.e., Mg-SPF+Sol-Gel and Mg-SPF+HT) showing osteogenic properties;
3. both kinds of Mg-based devices exhibited antibacterial properties, highly desirable in several biomedical applications.

However, further studies are needed to support and confirm the obtained results in an in vivo setting.

Funding

This study is supported by the project "CustOm-made aNTibacterial/bioActive/bioCoated prostheses" (CONTACT) - CUP: B19J20000490005.

Declaration of Competing Interest

The authors declared no potential conflicts of interest with respect to the research, authorship, and/or publication of this article.

Acknowledgments

We express our gratitude to Angela Cusanno from Politecnico di Bari for her invaluable technical support in the SPF forming technique, and to Agnese D'Agostino from Politecnico di Milano for her expertise and assistance in the Sol-Gel coating technique.

References

- Manam NS, Harun WS, Shri DNA, Ghani SAC, Kurniawan T, Ismail MH, et al. Study of corrosion in biocompatible metals for implants: a review. *J Alloy Compd* 2017; 701:698–715. <https://doi.org/10.1016/j.jallcom.2017.01.196>.
- Marrelli M, Pujia A, Palmieri F, Gatto R, Falisi G, Gargari M, et al. Innovative approach for the in vitro research on biomedical scaffolds designed and customized with CAD-CAM technology. *Int J Immunopathol Pharm* 2016;29:778–83. <https://doi.org/10.1177/0394632016646121>.
- Zhao D, Witte F, Lu F, Wang J, Li J, Qin L. Current status on clinical applications of magnesium-based orthopaedic implants: a review from clinical translational perspective. *Biomaterials* 2017;112:287–302. <https://doi.org/10.1016/j.biomaterials.2016.10.017>.
- Chen J, Tan L, Yu X, Etim IP, Ibrahim M, Yang K. Mechanical properties of magnesium alloys for medical application: a review. *J Mech Behav Biomed Mater* 2018;87:68–79. <https://doi.org/10.1016/j.jmbbm.2018.07.022>.
- Tan J, Ramakrishna S. Applications of magnesium and its alloys: a review. *Appl Sci* 2021;11:6861. <https://doi.org/10.3390/app1156861>.
- Marrelli M, Falisi G, Apicella A, Apicella D, Amantea M, Cielo A, et al. The behavior of dental pulp stem cells on different types of innovative mesoporous and nanoporous silicon scaffolds with different functionalizations of the surfaces. *J Biol Regul Homeost Agents* 2015;29:991–7.
- Alabort E, Putman D, Reed RC. Superplasticity in Ti–6Al–4V: characterisation, modelling and applications. *Acta Mater* 2015;95:428–42. <https://doi.org/10.1016/j.actamat.2015.04.056>.
- ISO 10993–5: biological evaluation of medical devices: tests for in vitro cytotoxicity. *International Organization of Standards*. 2009.
- Marrelli M, Paduano F, Tatullo M. Cells isolated from human periapical Cysts express mesenchymal stem cell-like properties. *Int J Biol Sci* 2013;9:1070–8. <https://doi.org/10.7150%2Fijbs.6662>.
- Choi SH, Jang YS, Jang JH, Bae TS, Lee SJ, Lee MH. Enhanced antibacterial activity of titanium by surface modification with polydopamine and silver for dental implant application. *2280800019847067 J Appl Biomater Funct Mater* 2019;17. <https://doi.org/10.1177/2280800019847067>.
- Wang QC, Zhang BC, Ren YB, Yang K. Research and application of biomedical nickel-free stainless steels. *Jinshu Xuebao* 2017;53:1311–6.
- Chen Q, Thouas GA. Metallic implant biomaterials. *Mater Sci Eng R Rep* 2015;87: 1–57. <https://doi.org/10.1016/j.mser.2014.10.001>.
- Kim HD, Amirthalingam S, Kim SL, Lee SS, Rangasamy J, Hwang NS. Biomimetic materials and fabrication approaches for bone tissue engineering. *Adv Health Mater* 2017;6:1700612. <https://doi.org/10.1002/adhm.201770120>.
- Wang C, Yi Z, Sheng Y, Tian L, Qin L, Ngai T, et al. Development of a novel biodegradable and anti-bacterial polyurethane coating for biomedical magnesium rods. *Mater Sci Eng C* 2019;99:344–56. <https://doi.org/10.1016/j.msec.2019.01.119>.
- Lee SY, Shrestha S, Shrestha BK, Park CH, Kim CS. Covalent surface functionalization of bovine serum albumin to magnesium surface to provide robust corrosion inhibition and enhance in vitro osteo-inductivity. *Polymers* 2020;12:439. <https://doi.org/10.3390/polym12020439>.
- Jing X, Ding Q, Wu Q, Su W, Yu K, Su Y, et al. Magnesium-based materials in orthopaedics: material properties and animal models. *Biomater Transl* 2021;2: 197–213. <https://doi.org/10.12336%2Fbiomatertransl.2021.03.004>.
- On SW, Cho SW, Byun SH, Yang BE. Bioabsorbable osteofixation materials for maxillofacial bone surgery: a review on polymers and magnesium-based materials. *Biomedicines* 2020;8:300. <https://doi.org/10.3390/biomedicines8090300>.
- Bollino F., Catauro M. Sol-Gel Technology to Prepare Advanced Coatings, Photoenergy and Thin Film Materials; John Wiley & Sons, Inc.: Hoboken, NJ, USA, 2019, 321–378.
- Maqsood MF, Raza MA, Ghauri FA, Rehman ZU, Ilyas MT. Corrosion study of graphene oxide coatings on AZ31B magnesium alloy. *J Coat Technol Res* 2020;17: 1321–9.
- Antoniac I, Miculescu F, Cotrut C. Controlling the degradation rate of biodegradable Mg–Zn–Mn alloys for orthopaedic applications by electrophoretic deposition of hydroxyapatite coating. *Materials* 2020;13:263. <https://doi.org/10.3390/ma13020263>.
- Wang ZX, Xu L, Zhang JW, Ye F, Lv WG, Xu C, et al. Preparation and degradation behaviour of composite bio-coating on ZK60 magnesium alloy using combined micro-arc oxidation and electrophoresis deposition. *Front Mater* 2020;7:190–204. <https://doi.org/10.3389/fmats.2020.00190>.
- Zhang J, Shang Z, Jiang Y, Zhang K, Li X, Ma M, et al. Biodegradable metals for bone fracture repair in animal models: a systematic review. *Regen Biomater* 2021; 8:rbaa047. <https://doi.org/10.1093/rb/rbaa047>.
- Lai Y, Li Y, Cao H, Long J, Wang X, Li L, et al. Osteogenic magnesium incorporated into PLGA/TCP porous scaffold by 3D printing for repairing challenging bone defect. *Biomaterials* 2019;197:207–19. <https://doi.org/10.1016/j.biomaterials.2019.01.013>.
- Ribitsch I, Baptista PM, Lange-Consiglio A, Melotti L, Patruno M, Jenner F, et al. Large animal models in regenerative medicine and tissue engineering: to do or not to do. *Front Bioeng Biotechnol* 2020;8:972. <https://doi.org/10.3389/fbioe.2020.00972>.
- Inchingolo F, Ballini A, Cagiano R, Inchingolo AD, Serafini M, De Benedittis M, et al. Immediately loaded dental implants bioactivated with platelet rich plasma (PRP) placed in maxillary and mandibular region. *Clin Ter* 2015. 166:e146–52. <https://doi.org/10.1177/1721727215578346>.
- Chen DI, Zhao M, Mundy GR. Bone morphogenetic proteins. *Growth Factors* 2004; 22:233–41. <https://doi.org/10.1080/08977190412331279890>.
- Perniconi B, Coletti D, Aulino P, Costa A, Aprile P, Santacrose L, et al. Muscle acellular scaffold as a biomaterial: effects on C2C12 cell differentiation and interaction with the murine host environment. *Front Physiol* 2014;5:354. <https://doi.org/10.3389/fphys.2014.00354>.
- Jiang Y, Wang B, Jia Z, Lu X, Fang L, Wang K, et al. Polydopamine mediated assembly of hydroxyapatite nanoparticles and bone morphogenetic protein-2 on magnesium alloys for enhanced corrosion resistance and bone regeneration. *J Biomed Mater A* 2017;105:2750–61. <https://doi.org/10.1002/jbm.a.36138>.
- Reible B, Schmidmaier G, Prokscha M, Moghaddam A, Westauser F. Continuous stimulation with differentiation factors is necessary to enhance osteogenic differentiation of human mesenchymal stem cells in-vitro. *Growth Factors* 2017; 35:179–88. <https://doi.org/10.1080/08977194.2017.1401618>.
- Liu Y, Wang Y, Sun X, Zhang X, Wang X, Zhang C, et al. RUNX2 mutation reduces osteogenic differentiation of dental follicle cells in cleidocranial dysplasia. *Mutagenesis* 2018;33:203–14. <https://doi.org/10.1093/mutage/gy010>.
- Yan G, Yuan Y, He M, Gong R, Lei H, Zhou H, et al. m6A methylation of precursor-miR-320/RUNX2 controls osteogenic potential of bone marrow-derived mesenchymal stem cells. *Mol Ther Nucleic Acids* 2020;19:421–36. <https://doi.org/10.1016/j.omtn.2019.12.001>.
- Rahim MI, Ullah S, Mueller PP. Advances and challenges of biodegradable implant materials with a focus on magnesium-alloys and bacterial infections. *Metals* 2018; 8:532. <https://doi.org/10.3390/met8070532>.
- Marrelli M, Tatullo M. Influence of PRF in the healing of bone and gingival tissues. *Clinical and histological evaluations. Eur Rev Med Pharmacol Sci* 2013;17: 1958–62.
- Tatullo M, Codispoti B, Paduano F, Nuzzolese M, Makeeva I. Strategic tools in regenerative and translational dentistry. *Int J Mol Sci* 2019;20:1879. <https://doi.org/10.3390/ijms20081879>.
- Wang M, Li H, Yang Y, Yuan K, Zhou F, Liu H, et al. A 3D-bioprinted scaffold with doxycycline-controlled BMP2-expressing cells for inducing bone regeneration and inhibiting bacterial infection. *Bioact Mater* 2021;6:1318–29. <https://doi.org/10.1016/j.bioactmat.2020.10.022>.
- Feng H, Wang G, Jin W, Zhang X, Huang Y, Gao A, et al. Systematic study of inherent antibacterial properties of magnesium-based biomaterials. *ACS Appl Mater Interfaces* 2016;8:9662–73. <https://doi.org/10.1021/acsami.6b02241>.
- Yazdimaghani M, Razavi M, Vashae D, Moharamzadeh K, Boccaccini AR, Tayebi L. Porous magnesium-based scaffolds for tissue engineering. *Mater Sci Eng C* 2017;71:1253–66. <https://doi.org/10.1016/j.msec.2016.11.027>.
- Grünwald TA, Rennhofer H, Hess B, Burghammer M, Stanzl-Tschegg SE, Cotte M, et al. Magnesium from bioresorbable implants: distribution and impact on the nano- and mineral structure of bone. *Biomaterials* 2016;76:250–60. <https://doi.org/10.1016/j.biomaterials.2015.10.054>.